Online Supplementary Information

A Self-Sustaining Ultra High Frequency Nanoelectromechanical Oscillator

X.L. Feng[1,2], C.J. White[2], A. Hajimiri[2], M.L. Roukes[1*]

[1]Kavli Nanoscience Institute, MC 114-36, and [2]Electrical Engineering, MC 136-93
California Institute of Technology, Pasadena, CA 91125, USA

[*]E-mail: roukes@caltech.edu

© 2008 **Nature Publishing Group**

From Open-Loop UHF NEMS Resonance Detection to Close-Loop Self Oscillation

Fig. S1 shows the circuit diagram for a self-sustaining UHF NEMS oscillator. As shown, open-loop measurements in the resonance-detection mode are made via two-port network analysis (transmission from port 1 to port 2) by employing a UHF/microwave network analyzer (HP8720C).

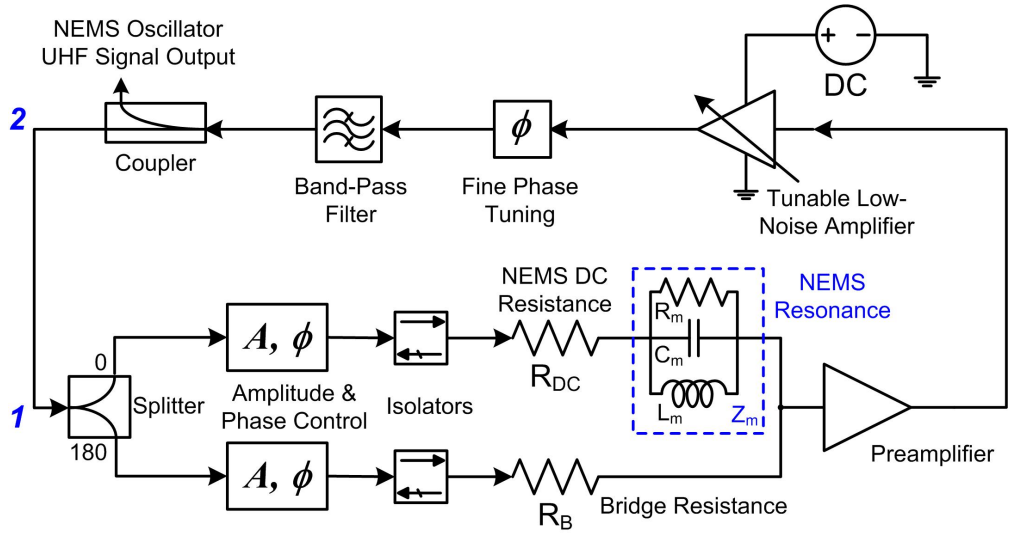

Figure S1 Circuit diagram for the demonstration and characterization of a self-sustaining UHF NEMS oscillator.

In open-loop operation, this finely-tunable bridge circuit[S1] can deeply null the background response arising from parasitic effects and impedance mismatch to yield excellent signal-to-background ratios (SBR's) of order ~5−10dB, on resonance. Various components for high-resolution 180-degree-phase bridging and background nulling are also illustrated in the circuit diagram. Here R_B is the resistance of a nanofabricated bridge resistor on chip (as shown in the inset of Fig. 1) – in practice it is often more convenient to employ another metalized nanobeam whose DC resistance is very close to the DC resistance of the resonator device of interest. This

© 2008 Nature Publishing Group

bridge nanobeam has also been made so that its resonance frequency is far enough from the resonance frequency of the resonator device of interest. Parasitic reflection and standing wave effects due to mismatch are efficiently reduced via directional signal isolation. Amplitude and phase in each branch of the bridge are precisely controlled by high-precision attenuators and delay lines. Both the loop gain and phase change can be finely tuned.

As demonstrated in Fig. S2, typical open-loop measurements of the UHF NEMS responses employing the circuit in Fig. S1 can yield SBR's of ~10dB. This represents a significant improvement over the SBR's of ~0.1–0.5dB typically obtained with the previous scheme[S2,S3].

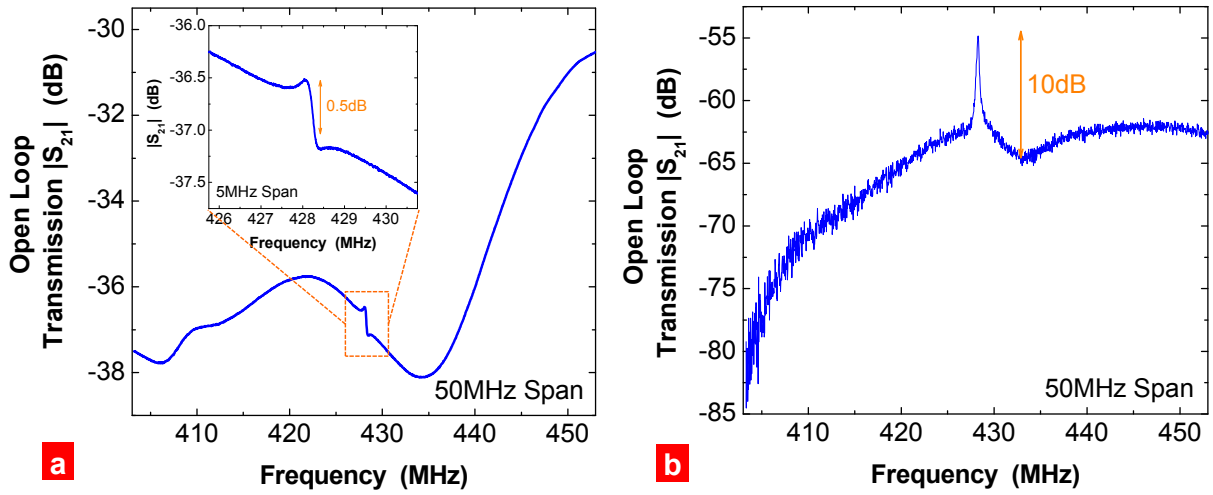

Figure S2 Open loop measurement of UHF NEMS resonance response (transmission $|S_{21}|$ between the nodes 1 and 2). **(a)** Small UHF resonance signal embedded in large, complex background response, measured by employing the scheme and circuit used in references [S2] and [S3]. **(b)** Significantly enhanced UHF resonance signal measured using the circuit shown in Fig. S1 in its open-loop mode (before applying feedback gain).

© 2008 Nature Publishing Group

Self-Sustaining UHF NEMS Oscillator Characterization

Fig. S3 demonstrates the open-loop calibration and adjustment of the loop gain and loop phase change to enable attainment of oscillation conditions dictated by the Barkhausen criterion[S4]. The open-loop measurements are performed by microwave network analysis between nodes 1 and 2 of the circuit. By setting the overall open-loop gain at the NEMS resonance frequency and its vicinity to be larger than 1 (*i.e.*, $|S_{21}| \geq 0$dB), and tuning the overall open-loop phase change to be $\phi(S_{21}) = 2n\pi$ (n is an integer), self-oscillation is realized when the loop is closed.

At stable self-oscillation, the frequency-domain oscillator output is characterized by using spectrum analyzer (HP8563E Spectrum Analyzer, 9kHz–26.5GHz). The time-domain oscillation waveforms are measured by employing a high-speed oscilloscope (Agilent Infinium 8000 Series Oscilloscope, 8GSa/s).

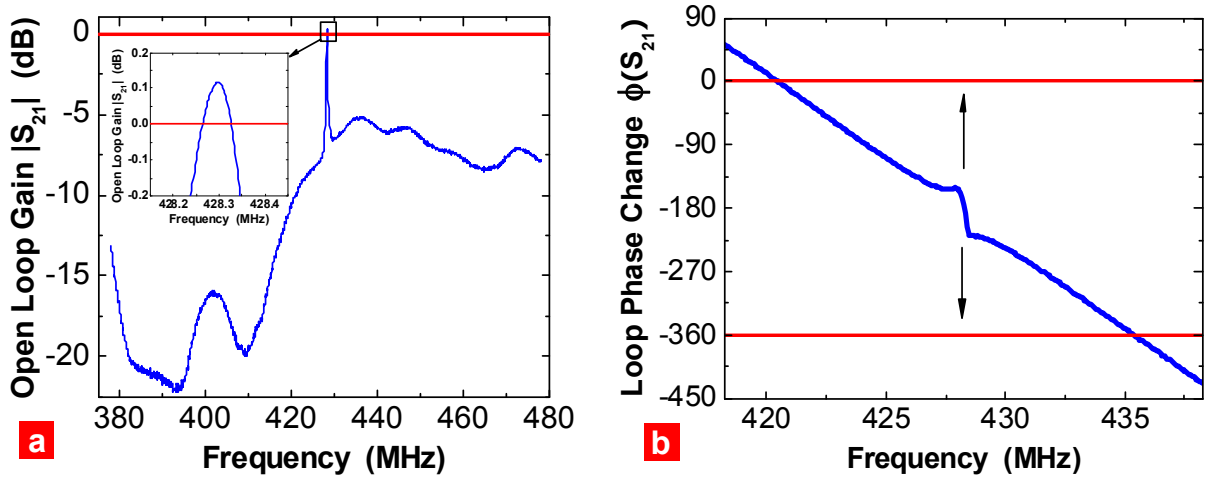

Figure S3 Open loop calibration and satisfying the Barkhausen criterion by adjusting **(a)** the open loop gain and **(b)** the loop phase change.

© 2008 Nature Publishing Group

NEMS Oscillator Phase Noise and Frequency Stability: Comparison and Ultimate Limits

This section supplements the discussion covered in the main text, on the phase noise performance of our UHF NEMS oscillator. Here we show again in Fig. S4 the measured phase noise data with the Leeson-type empirical fit[S4,S5,S6], and the ultimate performance of this NEMS oscillator as limited by the device's thermomechanical fluctuations[S7]. Moreover, we amend the plot by incorporating some data from state-of-the-art 13MHz quartz crystal oscillators[S8], for comparison.

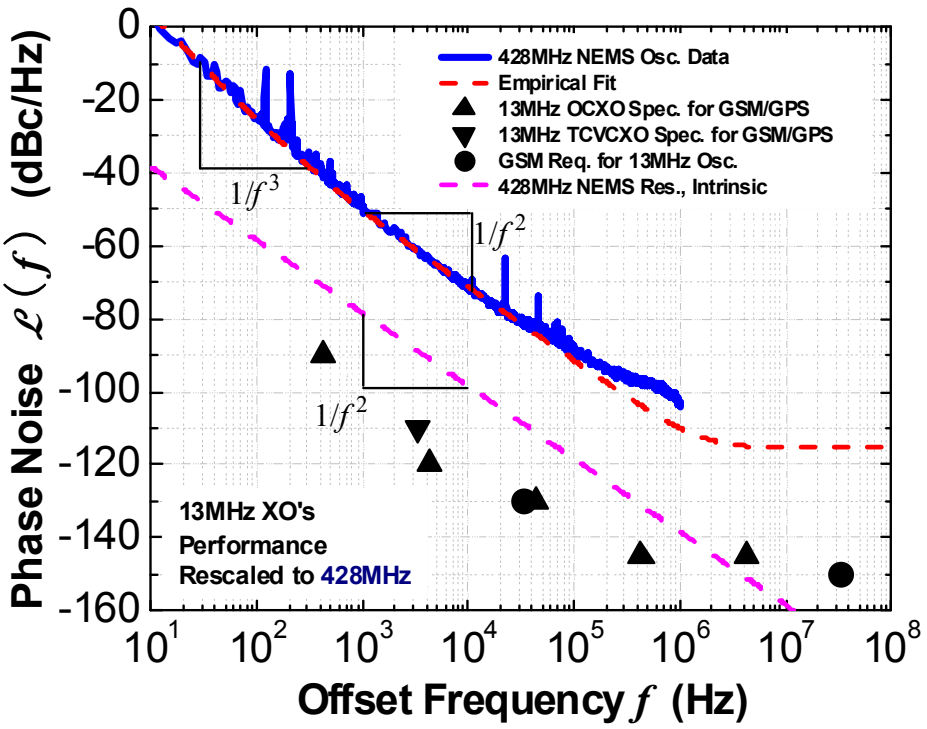

Figure S4 Phase noise performance of the UHF NEMS oscillator, in comparison with high-performance 13MHz quartz crystal oscillators (the phase noise performance is rescaled to the 428MHz carrier).

© 2008 Nature Publishing Group

As also demonstrated in Fig. S4, it is noteworthy that the intrinsic noise limits of the NEMS oscillators yield frequency stability approaching that of the state-of-the-art quartz crystal oscillators (XO's)[S8]. This suggests potential high-profile future applications for NEMS oscillators such as GSM/GPS communications. The phase noise performance of the present unoptimized, prototype NEMS oscillator already matches or surpasses the levels achieved by oscillators based on doubly-clamped beam MEMS resonators[S9]. MEMS oscillators based on much stiffer micromechanical modes, in structures such as wine-glass disk resonators[S9], film-bulk acoustic resonators (FBAR's)[S10], have now being engineered to approach the phase noise performance of macroscale quartz crystal oscillators[S11]. We note that such phase noise comparisons require rescaling of different oscillators' performance with respect to their carrier frequencies, so that a common figure of merit is evaluated and fairly compared[S1]. While the MEMS resonators can handle carrier signal power (P_C) in the range of ~0.1μW to ~1mW (for devices ranging from doubly-clamped beams to wine-glass disks and to FBAR's), the power handling of UHF NEMS resonators (doubly-clamped beams) is often in the range of P_C~0.1nW–100nW[S1]. We also note that in the comparison of phase noise performance in Fig. S4, the NEMS oscillator performance is associated with a lower temperature. At elevated temperatures, thermomechanical noise and Johnson noise rise but this temperature effect is minor; the amplifier noise is relatively temperature insensitive (determined by the amplifier's equivalent noise temperature or noise factor).

The ultimate, intrinsic phase noise limits for NEMS may also be attainable with advanced resonator designs to increase the device Q, and with the possible use of NEMS arrays to enhance power handling (P_C) and reduce noise. For example, a ten-fold improvement in Q, *i.e.*, to ~25,000 (assuming fixed resonance frequency and power handling) would yield $\langle \delta f_0 / f_0 \rangle_\tau$ ~

© 2008 Nature Publishing Group

5×10^{-11}. Such benefits may be achievable with optimization of mode-shape designs (*e.g.*, using stiffer modes and minimizing clamping losses) and advanced device processing techniques (*e.g.*, employing materials with ideally-terminated surfaces and ultralow internal friction, possibly also subjected to post-processing annealing or reflow).

In this work, the phase noise measurements are carried out using a specialized phase noise analyzer (RDL NTS-1000B Phase Noise Analyzer). The time-domain frequency stability characteristics are studied by using a high-precision frequency counter (Agilent 53132A Universal Counter, with UHF and high-precision options).

© 2008 **Nature Publishing Group**

References

S1. Feng, X.L. *Ph.D. Thesis*, California Institute of Technology (2007).

S2. Huang, X.M.H., Zorman, C.A., Mehregany, M. & Roukes, M.L. Nanodevice motion at microwave frequencies, *Nature* **421**, 496 (2003).

S3. Huang, X.M.H., Feng, X.L., Zorman, C.A., Mehregany, M. & Roukes, M.L. VHF, UHF and microwave frequency nanomechanical resonators, *New J. Phys.* **7**, 247 (2005).

S4. A. Hajimiri, T.H. Lee, *The Design of Low Noise Oscillators* (Kluwer Academic Publishers, Norwell, 1999).

S5. Lee, T.H. & Hajimiri, A. Oscillator phase noise: a tutorial, *IEEE J. Solid-State Circuits* **35**, 326-336 (2000).

S6. Leeson, D.B. A simple model of feedback oscillator noise spectrum, *Proc. IEEE* **54**, 329-330 (1966).

S7. Cleland, A.N. & Roukes, M.L. Noise processes in nanomechanical resonators, *J. Appl. Phys.* **92**, 2758-2769 (2002).

S8. Phase noise data and specifications of the state-of-the-art quartz crystal oscillators as frequency references are from Raltron (www.raltron.com). GSM stands for global system for mobile communication, and GPS stands for global positioning system. OCXO stands for oven-controlled crystal oscillator and TCVCXO stands for temperature-compensated and voltage-controlled oscillator. For a fair comparison, data from the 13MHz quartz crystal oscillators are rescaled up to 428MHz by normalizing offset frequency to carrier frequency.

S9. Lin, Y.W. *et al.* Series-resonant VHF micromechanical resonator reference oscillators, *IEEE J. Solid-State Circuits* **39**, 2477-2491 (2004).

S10. Otis, B.P. & Rabaey, J.M. A 300μW 1.9GHz CMOS oscillator utilizing micromachined resonators, *IEEE J. Solid-State Circuits* **38**, 1271-1274 (2003).

S11. Vig, J.R. & Kim, Y. Noise in microelectromechanical system resonators, *IEEE Trans. Ultrason. Ferroelectr. Freq. Contr.* **46**, 1558-1565 (1999).

© 2008 **Nature Publishing Group**